Article

Cite This: *Biomacromolecules* XXXX, XXX, XXX–XXX

pubs.acs.org/Biomac

# Injectable Polymer–Nanoparticle Hydrogels for Local Immune Cell Recruitment

Owen S. Fenton,[†,‡] Mark W. Tibbitt,[†,‡,§] Eric A. Appel,[†,‡,∥] Siddharth Jhunjhunwala,[†,‡,⊥] Matthew J. Webber,[†,‡,#] and Robert Langer*[,†,‡]

[†]Koch Institute for Integrative Cancer Research and [‡]Department of Chemical Engineering, Massachusetts Institute of Technology, Cambridge, Massachusetts 02142, United States

[§]Macromolecular Engineering Laboratory, Department of Mechanical and Process Engineering, ETH Zürich, Zürich 8092, Switzerland

[∥]Department of Materials Science and Engineering, Department of Bioengineering, Stanford University, Stanford, California 94305, United States

[⊥]Centre for BioSystems Science and Engineering, Indian Institute of Science, Bangalore 560012, India

[#]Department of Chemical and Biomolecular Engineering, University of Notre Dame, Notre Dame, Indiana 46556, United States

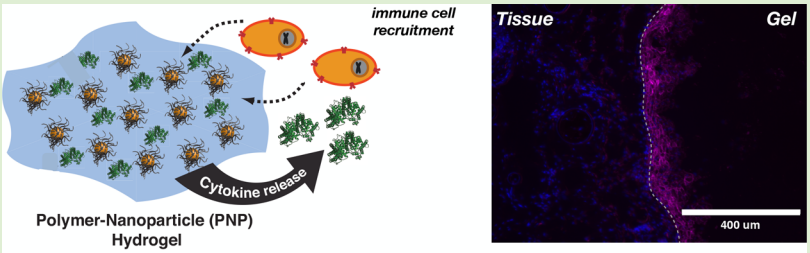


*Immune Cell Recruitment to the Site of Injection*

**ABSTRACT:** The ability to engineer immune function has transformed modern medicine, highlighted by the success of vaccinations and recent efforts in cancer immunotherapy. Further directions in programming the immune system focus on the design of immunomodulatory biomaterials that can recruit, engage with, and program immune cells locally in vivo. Here, we synthesized shear-thinning and self-healing polymer–nanoparticle (PNP) hydrogels as a tunable and injectable biomaterial platform for local dendritic cell (DC) recruitment. PNP gels were formed from two populations of poly(ethylene glycol)-*block*-polylactide (PEG-*b*-PLA) NPs with the same diameter but different PEG brush length (2 or 5 kDa). PEG-*b*-PLA NPs with the longer PEG brush exhibited improved gel formation following self-assembly and faster recovery after shear-thinning. In all cases, model protein therapeutics were released via Fickian diffusion in vitro, and minor differences in the release rate between the gel formulations were observed. PNP hydrogels were loaded with the DC cytokine CCL21 and injected subcutaneously in a murine model. CCL21-loaded PNP hydrogels recruited DCs preferentially to the site of injection in vivo relative to non-CCL21-loaded hydrogels. Thus, PNP hydrogels comprise a simple and tunable platform biomaterial for in vivo immunomodulation following minimally invasive subcutaneous injection.

## INTRODUCTION

The immune system is an organized and complex network of cells and processes that functions to protect the body from the threat of foreign substances.[1−3] Implantation of foreign materials often elicits a significant host immune response, which influences the fate and function of the designed biomaterial.[4] Therefore, a recent focus in the biomaterials field is to engineer immunomodulatory biomaterials that modulate the host immune response through materials design.[5] This paradigm adapts principles from native immune signaling to reprogram the immune response at the molecular or cellular level. This includes the design of immune-evasive or immune-privileged materials that mask the implanted material from rejection via the foreign body response. As an example, recent work from Anderson and co-workers has introduced alginate derivatives that evade immune detection and remain antifibrotic in the body.[6,7] In a complementary approach, immune-activating materials are being designed that specifically engage with the immune system to elicit a desired response.[3,8] As an example, Mooney and colleagues have developed surgically implanted, infection-mimicking materials that recruit dendritic cells (DCs), present tumor specific antigens to them, and stimulate antitumor immunity.[9]

Successful implementation of immunomodulatory materials requires engineered interactions with normal immune signaling to modulate the innate or adaptive immune response.[2] DCs are

Received: August 15, 2019
Revised: October 12, 2019

   DOI: 10.1021/acs.biomac.9b01129

the most potent antigen-presenting cells in the immune system and are central to the design of several immunomodulatory materials.[10] In a normal context, DCs interact with an antigen at the site of invasion of a foreign substance.[11] If the DCs are also presented with pro-inflammatory signals, they will mature phenotypically and migrate to lymph nodes, where they can stimulate naive T cells against the specific antigen.[12] Without an accompanying inflammatory signal, peripheral tolerance to the antigen can be induced. Therefore, immunomodulatory materials often seek to recruit and engage DCs.[2,11] Throughout, DCs migrate by chemotaxis in response to several cytokines, including CCL21 which attracts mature DCs to the afferent lymph in the skin.[13,14] Strategies that coapt normal cytokine-driven DC migration can be used to recruit DCs to an engineered biomaterial.[9]

An attractive immunomodulatory biomaterial platform would be applied in vivo in a facile manner, recruit specific immune cells (e.g., DCs) to the site of application and stimulate immune function. Initial designs of clinically relevant immunomodulatory materials have focused on surgically implantable solid devices composed of macroporous poly(lactide-*co*-glycolide).[9] This work has been extended to injectable immunomodulatory biomaterials that assemble in vivo from mesoporous silica rods.[15] Water swollen, cross-linked polymer networks or hydrogels provide a complementary approach for the design of cell recruitment biomaterials given their tunable mechanical properties, ability to provide controlled release of encapsulated molecules, and resemblance to soft biological tissue.[16−21] In addition, injectable hydrogels have been designed that flow as a viscous liquid under applied force (i.e., shear-thin) and reform into a viscoelastic gel upon cessation of the force by means of spontaneous reformation of the disrupted interactions (i.e., self-heal), making them advantageous for in vivo application as immunomodulatory materials that could be used as depots.[22] Indeed, such hydrogels can be applied in a minimally invasive manner through a standard percutaneous injection via facile flow through high gauge needles if the high shear viscosity is low.[22,23] In addition, rapid self-healing limits the burst release of entrapped therapeutics, which is observed with some phase inversion or thermosetting injectable hydrogels.[24]

Here, we synthesize a class of shear-thinning and self-healing hydroxypropylmethylcellulose (HPMC) polymer−nanoparticle (PNP) hydrogels with the intent to design an injectable biomaterial for cytokine release and recruitment of DCs. Two populations of poly(ethylene glycol)-*block*-polylactide (PEG-*b*-PLA) nanoparticles (NPs) (a class of biocompatible and biodegradable NPs employed as drug delivery vehicles in a range of applications) were synthesized with the same diameter ($D_h \approx 80$ nm), which is small enough to encourage gel formation by virtue of favoring polymer bridging of multiple NPs as opposed to the wrapping of polymers around individual particles,[25] but different PEG brush lengths (2 or 5 kDa). PNP gels were formulated from both NPs, and gels composed of NPs with the longer PEG brush exhibited improved rheological properties and faster recovery after shear-thinning. Model protein therapeutics were released from the gels over the course of ∼1 week in vitro and ∼5 days in vivo. Minor differences in the release rate between the gel formulations were observed. PNP gels were loaded with CCL21 and injected subcutaneously in a murine model. CCL21-loaded PNP gels recruited $CD11^+$ DCs preferentially to the site of injection in vivo relative to non-CCL21-loaded hydrogels.

## MATERIALS AND METHODS

**Techniques and Materials.** $^1$H NMR (400 MHz) spectra were recorded using Bruker AVANCE QNP 400. Chemical shifts are recorded in ppm ($\delta$) in $H_2O$ with the internal reference set to $\delta$ = 4.80 ppm. Attenuated total reflectance-Fourier transform infrared spectroscopy was performed using a PerkinElmer Spectrum 100 series FT-IR spectrometer equipped with a universal ATR sampling accessory. Gel permeation chromatography (GPC) was performed in tetrahydrofuran (THF) on a divinylbenzene column utilizing a Malvern ViscotekTM TDA305 triple detection system. Samples were filtered over 0.2 $\mu$m polytetrafluoroethylene filters before injection and the GPC was conducted with a flow rate of 1.0 mL/min. Molecular weights and polydispersities were determined by comparing to poly(methyl methacrylate) standards. Dynamic light scattering (DLS) measurements were performed with a Malvern Instruments Zetasizer Nano-ZS. All animal studies were approved by the MIT Institutional Animal Care and Use Committee and were consistent with local, state, and federal regulations as applicable.

Rheological characterization was performed using a TA Instruments AR-G2 stress-controlled rheometer fitted with a Peltier stage set to 37 °C. Dynamic oscillatory strain amplitude sweep measurements were conducted at a frequency of 10 rad/s (unless otherwise noted). Dynamic oscillatory frequency sweep measurements were conducted at a 2% strain amplitude (unless otherwise noted). All measurements were performed using a 20 mm 4° cone-plate geometry and analyzed using TA Instruments TRIOS software.

Monomethoxy-poly(ethylene glycol) (PEG; 2 or 5 kDa) was purchased from Aldrich and was purified by azeotropic distillation with toluene. Lactide (LA) was purchased from Aldrich, recrystallized from ethyl acetate, and dried in a desiccator over $P_2O_5$ prior to use. All other materials were purchased from Aldrich (except as noted) and used as received.

**Procedures.** *Synthesis of HPMC-$C_{12}$.* HPMC (1.0 g) was dissolved in *N*-methylpyrrolidone (NMP; 45 mL) by stirring at 80 °C for 1 h. The solution was cooled to room temperature and a solution of 1-dodecylisocyanate (0.5 mmol) and triethylamine (50 $\mu$L) dissolved in NMP (5 mL) was added to the reaction mixture. The reaction was then stirred at room temperature for 16 h. Following reaction, the functionalized HPMC was precipitated from acetone and recovered by filtration. Following precipitation, the functionalized HPMC was dissolved in deionized water (0.5 wt %) and dialyzed against deionized water (Spectra/Por 7 Dialysis Membrane, Pre-treated RC tubing; 10 kDa MWCO; SpectrumLabs, Inc.) for 5 days. The functionalized HPMC solution was then lyophilized, yielding the functionalized HPMC (HPMC-$C_{12}$) as white powder. FT-IR: $\nu$ = 1685, 1601, 1367 cm$^{-1}$.

*Synthesis of PEG-b-PLA block Copolymers.* For the synthesis of $PEG_{5k}$-*b*-$PLA_{20k}$, PEG ($M_n \approx 5$ kDa, 0.25 g, 4.1 mmol) and 1,8-diazabicycloundec-7-ene (DBU; 10.6 mg, 10 $\mu$L, 1.0 mol % relative to LA) were dissolved in dichloromethane (DCM) (1.0 mL). LA (1.0 g, 6.9 mmol) was dissolved in DCM (3.0 mL) with mild heating. The LA solution was added to the PEG/DBU solution and was allowed to stir for 10 min. For the synthesis of $PEG_{2k}$-*b*-$PLA_{16k}$, PEG ($M_n \approx 2$ kDa, 0.25 g, 4.1 mmol) and 1,8-diazabicycloundec-7-ene (DBU; 10.6 mg, 10 $\mu$L, 1.0 mol % relative to LA) were dissolved in DCM (1.0 mL). LA (1.0 g, 6.9 mmol) was dissolved in DCM (3.0 mL) with mild heating. The LA solution was added to the PEG/DBU solution and was allowed to stir for 10 min. In each case, the reaction mixture was quenched by addition of acetone (∼7.0 mL) and the PEG-*b*-PLA copolymer was recovered by precipitation from cold diethyl ether, collected by filtration, and dried under vacuum (24−48 h) to yield a white polymer. GPC (THF): $PEG_{5k}$-*b*-$PLA_{20k}$ measured as $M_n$ ($Đ$) = 25 kDa (1.09). $PEG_{2k}$-*b*-$PLA_{16k}$ measured as $M_n$ ($Đ$) = 19 kDa (1.13).

*Nanoprecipitation of PEG-b-PLA NPs.* $PEG_{5k}$-*b*-$PLA_{20k}$ (50 mg) was dissolved in dimethylsulfoxide (1 mL) with mild heating and agitation. Deionized water (10 mL) was added to a 20 mL scintillation vial and stirred with a magnetic stir bar on a stir plate. The $PEG_{5k}$-*b*-$PLA_{20k}$ solution was added dropwise to the stirring water to nanoprecipitate $PEG_{5k}$-*b*-$PLA_{20k}$ NPs. A small portion of the


DOI: 10.1021/acs.biomac.9b01139

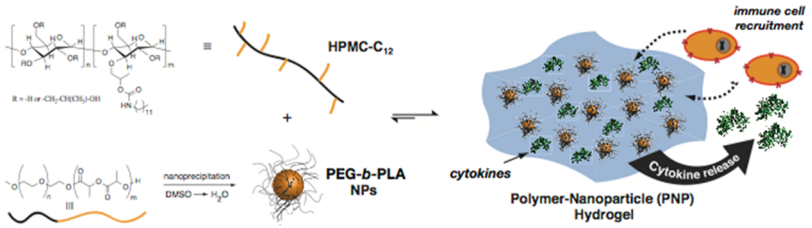


**Figure 1.** Schematic representation of PNP hydrogels comprising hydrophobically modified hydroxypropylmethylcellulose (HPMC-$C_{12}$) and PEG-*b*-PLA NPs. Investigations into the effect of block size on the material and release profiles of the PNP system as well as in vivo immune cell recruitment were explored in this work.

NPs were analyzed by DLS to determine size. NPs were purified by ultracentrifugation (4500 rcf) over a filter (Millipore Amicon Ultra-15; 10 kDa MWCO). Recovered NPs were resuspended in deionized water at a final concentration of 150 mg $mL^{-1}$. An identical formulation, isolation, and characterization procedure was performed to form $PEG_{2k}$-*b*-$PLA_{16k}$ NPs. $PEG_{2k}$-*b*-$PLA_{16k}$ and $PEG_{5k}$-*b*-$PLA_{20k}$ produced NPs of similar diameter ($D_h \approx 80$ nm) as determined by DLS (Malvern).

*Preparation of Self-Assembled Hydrogels.* HPMC-$C_{12}$ was dissolved overnight in deionized water at 3.0 wt % on a shaker plate. PEG-*b*-PLA NPs were prepared at 15.0 wt % in deionized water. To prepare polymer−nanoparticle hydrogels (PNP gels), HPMC-$C_{12}$ solutions were combined with NP solutions to a final weight fraction of 1 wt % HPMC-$C_{12}$: 1−10 wt % NPs. Final gels were prepared at 1.0 wt % HPMC-$C_{12}$ and 5.0 or 10 wt % PEG-*b*-PLA NPs. For 1.0:5.0 wt % gels, equal parts of HPMC-$C_{12}$ solution, NP solution, and deionized water were combined in a 1.7 mL microcentrifuge tube. For 1.0:10.0 wt % gels, one part HPMC-$C_{12}$ solution and two parts NP solution were combined in a 1.7 mL microcentrifuge tube. PNP gels were mixed well by vortex, mild centrifugation, and agitation to enable homogenization and removal of bubbles. For rheometry, 450 $\mu$L gels were prepared.

*In Vitro Protein Release from Hydrogels.* To investigate encapsulation and release of a model protein, hydrogels were prepared as described above with fluorescein isothiocyanate (FITC)-labeled bovine serum albumin (BSA) dissolved with the HPMC-$C_{12}$ polymer, resulting in a final concentration of FITC-BSA of 1.0 wt % in the gel. FITC-BSA loaded hydrogel (300 $\mu$L) was placed into a 1.7 mL microcentrifuge tube and deionized water (1 mL) was gently added on top of the hydrogel. This setup was placed into an incubator at 37 °C, and 0.8 mL of the aqueous supernatant solution was replaced with fresh deionized water at predetermined time intervals. In vitro release experiments were performed in triplicate. The collected aqueous solutions were analyzed for solute concentration based on calibration curves prepared using either FITC-BSA absorbance.

Modeling of the controlled release of drugs and other cargo from these polymeric devices has been a subject of considerable research. Many models in the past have focused on Fickian diffusion, however, Peppas and co-workers have derived an important and simple exponential relationship to describe the general release behavior of cargo from a polymeric device: $M_t/M_\infty = kt^n$, where $k$ is the release rate and $n$ is the release coefficient. The release coefficient is an indicator of the mode of release from the materials, where pure Fickian diffusional release is described by $n = 0.5$, with $n > 0.5$ revealing a greater contribution of "anomalous" release (caused by swelling or hydrogel erosion) to the overall release profile. We fit the FITC-BSA release data with this equation and determined that $n = 0.5$, highlighting that the BSA release is diffusional with a release rate of $k = 19\%/h^{0.5}$.

*In Vivo Protein Release from Hydrogels.* PNP gels were prepared with BSA-Alexa Fluor 647 (AF-BSA; 10 $\mu$M in the final gel; Life Technologies) loaded into the aqueous phase. Adult male SKH1E mice (8 weeks old) were injected subcutaneously on the back with the respective PNP gel formulations using a 26G syringe. For in vivo imaging, 8-week-old male hairless SKH1E mice were first maintained on an alfalfa-free diet for 2 weeks prior to administration to limit background fluorescence. Mice were anesthetized using inhaled isoflurane, and 200 $\mu$L of sample was injected subcutaneously into the rear right flank of the animal using a 26G syringe. Treatment groups consisted of the hydrogel with the AF-BSA ($n = 5$) and a bolus injection of AF-BSA in PBS ($n = 1$). Imaging was conducted on an IVIS Spectrum in vivo imaging system with a heated stage and an inhaled isoflurane manifold. Fluorescent images were collected at several time points over the following week, using filter sets of 675/720 (AF-680) with a 1.5 cm subject height using small binning and an F-stop of 1.

*Immune Cell Recruitment In Vivo by Controlled Cytokine Release.* PNP gels were prepared with either 0, 1, or 10 $\mu$g $mL^{-1}$ of CCL21 loaded into the aqueous phase. Adult mice were injected subcutaneously with 200 $\mu$L of the respective PNP gel formulations using a 26G syringe ($n = 5$). After 3 or 7 days, the mice were euthanized, and histological sectioning and staining for DCs were performed. Specifically, tissue sections were treated with 500 $\mu$L of 2% paraformaldehyde. After 20 min, the fixative was aspirated, the tissue sections were washed once with 500 $\mu$L of PBS containing 1% BSA, and then were treated for 1 h with an additional 500 $\mu$L of PBS containing 1% BSA at 4 °C. The buffer was aspirated, and then, 250 $\mu$L of the appropriate staining buffers as well as 4′,6-diamidino-2-phenylindole (DAPI) was then added [CD4—Alexa-488 (1:100 dilution); CD8a—Alexa 594 (1:100 dilution); CD11c—Alexa-647 (1:100 dilution)]. After 1 h incubation at 4 °C, the tissue sections were washed 5× with buffer and imaged.

## RESULTS AND DISCUSSION

First, we synthesized the molecular components required for PNP hydrogel formulation: a hydrophobically modified dodecyl HPMC derivative (HPMC-$C_{12}$, synthesized and selected for use as previously described)[25] and PEG-*b*-PLA polymers of distinct block molecular weights (namely, $PEG_{2k}$-*b*-$PLA_{16k}$ and $PEG_{5k}$-*b*-$PLA_{20k}$, synthesized as previously described) (Figure 1).[25,26] Each resultant batch of PEG-*b*-PLA was then formulated into NPs via nanoprecipitation (Figure 1).[27−29] $PEG_{2k}$-*b*-$PLA_{16k}$ and $PEG_{5k}$-*b*-$PLA_{20k}$ produced NPs of similar diameter ($D_h \approx 80$ nm) as determined by DLS. This diameter was selected for study because it is small enough to encourage gel formation by virtue of favoring polymer bridging of multiple NPs as opposed to the wrapping of polymers around individual particles.[25] Moreover, these polymers were designed such that the hydrodynamic size would be the same despite the change in the molecular weight of the PEG brush, allowing us to investigate the specific influence of the PEG block on PNP gel properties.

After synthesizing the required components, we then investigated PNP hydrogel formulation and rheological characterization. HPMC-$C_{12}$ (1 wt %) was combined with each of the aforementioned PEG-*b*-PLA NPs at either 5 or 10 wt % to generate a series of four PNP gels: (i) 1.0 wt % HPMC-$C_{12}$ + 5.0 wt % $PEG_{2k}$-*b*-$PLA_{16k}$ NPs; (ii) 1.0 wt %


DOI: 10.1021/acs.biomac.9b01139

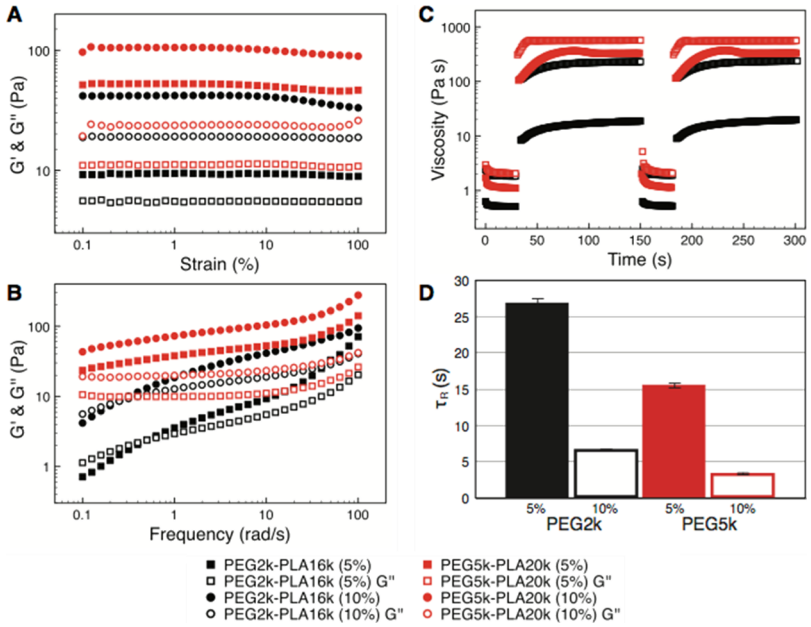


**Figure 2.** Oscillatory rheological characterization of PNP hydrogels comprised of HPMC-$C_{12}$ and PEG-*b*-PLA NPs of varied block sizes. (A) Strain-dependent rheological characterization. (B) Frequency-dependent rheological characterization. (C) Healing and recovery times for representative hydrogel formulations (D) fitting of step-rate time-sweep measurements to a single-stage association model ($R^2 > 0.95$) yields a characteristic time for recovery ($T_R$) of the hydrogel structure.

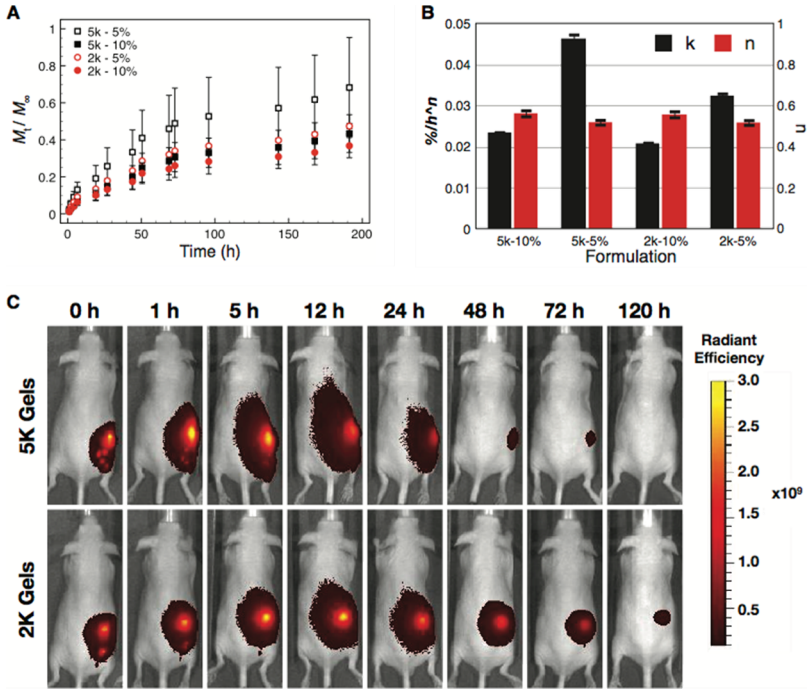


**Figure 3.** In vitro and in vivo model drug release from PNP hydrogel formulations. (A) In vitro drug release profile of FITC-BSA from PNP hydrogels showing the cumulative proportion of "drug" released [$M_t/M_\infty$; the cumulative fractional mass released at time $t$ ($n = 3$)]. (B) Fitting of the release data with the Ritger–Peppas equation provides the release coefficients ($k$) and the release exponent ($n$) for each hydrogel formulation. (C) Intravital imaging of the release of AF-BSA from the 0 wt % $PEG_{5k}$-*b*-$PLA_{20k}$ NP and $PEG_{2k}$-*b*-$PLA_{16k}$ NP formulations.

HPMC-$C_{12}$ + 10.0 wt % $PEG_{2k}$-*b*-$PLA_{16k}$ NPs; (iii) 1.0 wt % HPMC-$C_{12}$ + 5.0 wt % $PEG_{5k}$-*b*-$PLA_{20k}$ NPs; and (iv) 1.0 wt % HPMC-$C_{12}$ + 10.0 wt % $PEG_{5k}$-*b*-$PLA_{20k}$ NPs. The formulations will be referred to as 2k-5%, 2k-10%, 5k-5%, and 5k-10%, referring to the length of the PEG block and the weight percent of the NPs, respectively. Each of the four formulations resulted in gel formation upon mixing of the liquid solutions of HPMC-$C_{12}$ and NPs as determined by shear rheometry (tan $\delta < 1$; $\omega = 10$ rad $s^{-1}$, $\gamma = 1\%$).

We assessed the strain and frequency-dependent rheology of each of the four hydrogels on a stress-controlled shear rheometer (Figure 2). Our initial hypothesis was that NPs with a PEG block of lower molecular weight would result in gels with an increased plateau modulus, as the hydrophobic


DOI: 10.1021/acs.biomac.9b01139

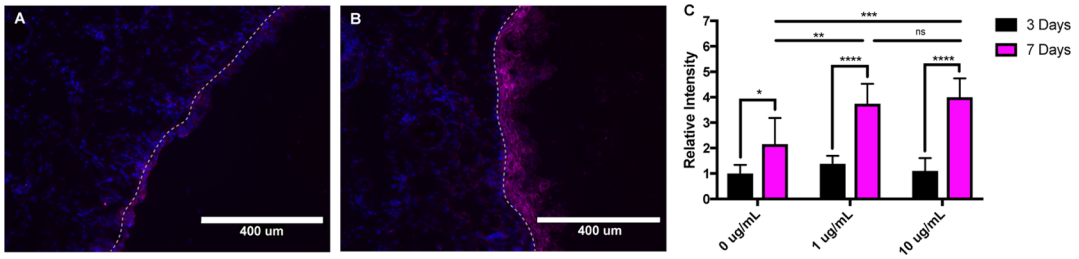


**Figure 4.** Localized recruitment of DCs into a subcutaneously injected cytokine-free or CCL21-impregnated PNP hydrogel. (A) Representative histological image of a resected cytokine-free hydrogel ($t$ = 7 days) demonstrating minimal infiltration of DCs (blue = DAPI, purple = anti-CD11c Alexa Fluor 647). Dashed line represents the border between tissue (left of dashed line) and the PNP hydrogel (right of dashed line). (B) Representative histological image of a resected CCL21-impregnated PNP hydrogel ($t$ = 7 days), demonstrating DC infiltration into the network (blue = DAPI, purple = anti-CD11c Alexa Fluor 647). Dashed line represents the border between tissue (left of dashed line) and the PNP hydrogel (right of dashed line). (C) Quantification of DC infiltration into cytokine-free and CCL21-impregnated PNP hydrogels at 3 and 7 day time points.

core of NPs should be more accessible to the HPMC-$C_{12}$. However, the plateau modulus ($\gamma$ = 0.1−10%; $\omega$ = 10 rad $s^{-1}$) for both the 2k-5% and 2k-10% gels had a lower plateau modulus as compared to 5k-5% and 5k-10% (Figure 2A). Furthermore, the 2k-5% and 2k-10% exhibited a crossover frequency $\omega_c \approx 0.5$ rad $s^{-1}$, whereas the crossover frequency for the 5k-5% and 5k-10% gels were both below 0.1 rad $s^{-1}$ (Figure 2B). This rheology indicates a weaker binding between the 2k NPs and the HPMC-$C_{12}$, refuting the initial hypothesis. In fact, these data suggest that entropic driving forces may influence the binding interaction between HPMC-$C_{12}$ and NPs, which would be favored with higher molecular weight PEG brushes. Future work will further investigate the mechanism of PNP gel formation.

The shear-thinning, self-healing, and recovery times for the PNP gels were also investigated by shear rheometry (Figure 2C,D). In all cases, the gels exhibited shear-thinning and self-healing behavior. At low strain ($\gamma$ = 0.1%), simulating the gel at rest on the lab bench, the gels exhibit high viscosity, indicative of the gel state; however, upon application of high strain ($\gamma$ = 500%) the gels thin and behave like a viscous liquid. Upon cessation of high strain, the gels heal rapidly back to the resting viscosity. These data indicate that the PNP gel platform can be used as an injectable biomaterial for local deployment via syringe injection.[23] A single-stage association model was used to fit for a characteristic time for recovery ($\tau_R$) of mechanical properties (Figure 2D). The recovery time was shorter for gels with 10 wt % NPs independent of PEG molecular weight and the 5k-10% gel demonstrated the fastest recovery ($\tau_R$ = 4.0 s). Consistent with previous reports, higher NP wt % increased the mechanical properties of the PNP gels.[25,30] We also found here that the recovery time was faster (i.e., lower) for gels with higher NP wt %, which may be due to an increased probability of cross-linking events. The higher molecular weight PEG block increased the mechanical properties of the PNP gels and led to faster (i.e., lower) recovery times.

Toward the aim of designing an injectable material to release compounds and recruit immune cells, we characterized the controlled release of macromolecules from PNP gels in vitro and in vivo. Each of the four gel formulations were loaded with FITC-BSA, which served as a readily quantifiable model protein payload that could be standardized relative to other systems.[31] The release of FITC-BSA from each of the gels was then determined via fluorescence quantification of the supernatant solution at defined time points (Figure 3A). The release curves for each formulation were modeled using the Ritger−Peppas equation $M_t/M_\infty = kt^n$, where $k$ is the release rate and $n$ is the release coefficient (Figure 3B).[32] All of the gel formulations released FITC-BSA via Fickian diffusion as indicated by the release coefficient $n \approx 0.5$ for each sample.[32] In addition, the release rate $k$ did not vary significantly between the different gel formulations with a slightly faster release for gels with 5 wt % NPs as compared to 10 wt % NPs. In total, FITC-BSA was released in vitro for ∼1 week from the PNP gel formulations. Future work will aim to further elucidate the mechanistic underpinnings behind these findings. Model in vivo release studies were also performed using the 5k-10% and 2k-10% formulations. These formulations were chosen for in vivo study so that the effect of NP block size on PNP delivery properties could be investigated; moreover, these two formulations formed more robust gels as compared to the 5k-5% and 2k-5% gels. Alexa Fluor-647-conjugated BSA (AF-BSA) was encapsulated in the 5k-10% and 2k-10% formulations, which were subsequently injected subcutaneously into adult SKH1E (hairless) mice. Intravital imaging revealed that BSA was released in vivo from the gels over the course of ∼120 h with the majority of the release occurring within the first 48 h (Figure 3C).

Finally, we investigated the ability of PNP gel formulations to recruit immune cell populations to the site of injection within the body. Cytokine injections and cytokine-impregnated implants have been successfully employed for localized immune cell recruitment in vivo with application in cellular activation for immunooncology as well as immune-cell mediated wound healing.[3,33] Although injections are simple to implement, their biological effects can be short-lived; by contrast, implants can recruit immune cells for sustained periods of time but require surgical methods for in vivo implementation. We therefore envisioned that developing a cytokine-impregnated variant of the PNP gel could combine the benefits of injection and implant-based immune-cell recruitment strategies, wherein sustained cytokine release profiles could be used to recruit immune cells following a single needle-based injection into the body (Figure 1).

To achieve this goal, we hypothesized that we could load a representative PNP formulation with C−C motif ligand 21 (CCL21), which promotes DC migration.[34] Our interest in recruiting DCs lies in the fact that they can be primed for antigen presentation to elicit antigen-specific T cell and antibody responses against a target of choice, an important property which renders them ideal targets for biomaterials research.[12] Indeed, recent efforts have already successfully demonstrated that DCs can be successfully recruited to, and activated within, sustained-release biomaterials scaffold to


DOI: 10.1021/acs.biomac.9b01139

mount an antigen specific T cell response.[15] Building upon these concepts, we first generated three discrete PNP formulations based upon the 5k-10% formulation (which was selected as the base formulation because it exhibited a frequency crossover below 0.1 rad/s and a robust storage moldulus of ∼100 Pa)—first, a cytokine free hydrogel formulation; second, a hydrogel formulation containing 1 $\mu$g mL$^{-1}$ of CCL21; and third, a hydrogel formulation containing 10 $\mu$g mL$^{-1}$ CCL21. Each of these formulations were then injected subcutaneously into C57BL/6 mice. After 3 or 7 days, the hydrogels were removed, processed for histology, stained with antibodies against DCs, and imaged to assess infiltration into the injected gel (Figure 4A,B); the concentrations contained within each gel was also quantified (Figure 4C). In analyzing these data, several trends are apparent: (i) injection of the empty hydrogel induces an immunological response, with cellular accumulation increasing most after 7 days; (ii) after 7 days, both CCL21 hydrogel formulations recruit a greater number of cells than the empty hydrogel alone; and (iii) no significant difference is observed between the 1 and 10 $\mu$g mL$^{-1}$ formulations in terms of recruitment. These observations indicate that it is possible to recruit DCs locally with this cytokine impregnation approach, a finding that furthers the application repertoire of PNP hydrogels for immunonoengineering approaches.

## CONCLUSIONS

In summary, we have developed a PNP hydrogel system capable of recruiting specific immune cell populations to the site of injection. In doing so, therefore, we hope to have furthered the utility of this biomaterials platform and provided generalizable strategies toward understanding and exploiting immune cell recruitment for biomaterials application. Future work will aim to build upon these findings by incorporating activating agents within the hydrogel to illicit targeted immunological responses in vivo in a minimally invasive fashion.

## AUTHOR INFORMATION


### Corresponding Author

*E-mail: rlanger@mit.edu (R.L.).

### ORCID

Mark W. Tibbitt: 0000-0002-4917-7187
Eric A. Appel: 0000-0002-2301-7126
Siddharth Jhunjhunwala: 0000-0001-8046-2288
Matthew J. Webber: 0000-0003-3111-6228
Robert Langer: 0000-0003-4255-0492


### Notes

The authors declare no competing financial interest.

## REFERENCES


(1) Ratner, B. D.; Hoffman, A. S.; Schoen, F. J.; Lemons, J. E., *Biomaterials Science: An Introduction to Materials in Medicine*; Academic Press, 2012.

(2) Hubbell, J. A.; Thomas, S. N.; Swartz, M. A. Materials engineering for immunomodulation. *Nature* **2009**, *462*, 449−460.

(3) Fenton, O. S.; Olafson, K. N.; Pillai, P. S.; Mitchell, M. J.; Langer, R. Advances in Biomaterials for Drug Delivery. *Adv. Mater.* **2018**, *30*, 1705328.

(4) Anderson, J. M. Biological Responses to Materials. *Annu. Rev. Mater. Res.* **2001**, *31*, 81−110.

(5) Lewis, J. S.; Roy, K.; Keselowsky, B. G. Materials that harness and modulate the immune system. *MRS Bull.* **2014**, *39*, 25−34.

(6) Vegas, A. J.; Veiseh, O.; Gürtler, M.; Millman, J. R.; Pagliuca, F. W.; Bader, A. R.; Doloff, J. C.; Li, J.; Chen, M.; Olejnik, K.; Tam, H. H.; Jhunjhunwala, S.; Langan, E.; Aresta-Dasilva, S.; Gandham, S.; McGarrigle, J. J.; Bochenek, M. A.; Hollister-Lock, J.; Oberholzer, J.; Greiner, D. L.; Weir, G. C.; Melton, D. A.; Langer, R.; Anderson, D. G. Long-term glycemic control using polymer-encapsulated human stem cell-derived beta cells in immune-competent mice. *Nat. Med.* **2016**, *22*, 306−311.

(7) Vegas, A. J.; Veiseh, O.; Doloff, J. C.; Ma, M.; Tam, H. H.; Bratlie, K.; Li, J.; Bader, A. R.; Langan, E.; Olejnik, K.; Fenton, P.; Kang, J. W.; Hollister-Locke, J.; Bochenek, M. A.; Chiu, A.; Siebert, S.; Tang, K.; Jhunjhunwala, S.; Aresta-Dasilva, S.; Dholakia, N.; Thakrar, R.; Vietti, T.; Chen, M.; Cohen, J.; Siniakowicz, K.; Qi, M.; McGarrigle, J.; Graham, A. C.; Lyle, S.; Harlan, D. M.; Greiner, D. L.; Oberholzer, J.; Weir, G. C.; Langer, R.; Anderson, D. G. Combinatorial hydrogel library enables identification of materials that mitigate the foreign body response in primates. *Nat. Biotechnol.* **2016**, *34*, 345−352.

(8) Wang, H.; Mooney, D. J. Biomaterial-assisted targeted modulation of immune cells in cancer treatment. *Nat. Mater.* **2018**, *17*, 761−772.

(9) Ali, O. A.; Huebsch, N.; Cao, L.; Dranoff, G.; Mooney, D. J. Infection-mimicking materials to program dendritic cells in situ. *Nat. Mater.* **2009**, *8*, 151−158.

(10) Chen, D. S.; Mellman, I. Oncology meets immunology: the cancer-immunity cycle. *Immunity* **2013**, *39*, 1−10.

(11) Steinman, R. M.; Banchereau, J. Taking dendritic cells into medicine. *Nature* **2007**, *449*, 419−426.

(12) Banchereau, J.; Steinman, R. M. Dendritic cells and the control of immunity. *Nature* **1998**, *392*, 245−252.

(13) Alvarez, D.; Vollmann, E. H.; von Andrian, U. H. Mechanisms and consequences of dendritic cell migration. *Immunity* **2008**, *29*, 325−342.

(14) Kabashima, K.; Shiraishi, N.; Sugita, K.; Mori, T.; Onoue, A.; Kobayashi, M.; Sakabe, J.-i.; Yoshiki, R.; Tamamura, H.; Fujii, N.; Inaba, K.; Tokura, Y. CXCL12-CXCR4 engagement is required for migration of cutaneous dendritic cells. *Am. J. Pathol.* **2007**, *171*, 1249−1257.

(15) Kim, J.; Li, W. A.; Choi, Y.; Lewin, S. A.; Verbeke, C. S.; Dranoff, G.; Mooney, D. J. Injectable, spontaneously assembling, inorganic scaffolds modulate immune cells in vivo and increase vaccine efficacy. *Nat. Biotechnol.* **2015**, *33*, 64−72.

(16) Lutolf, M. P.; Hubbell, J. A. Synthetic biomaterials as instructive extracellular microenvironments for morphogenesis in tissue engineering. *Nat. Biotechnol.* **2005**, *23*, 47−55.

(17) Appel, E. A.; del Barrio, J.; Loh, X. J.; Scherman, O. A. Supramolecular polymeric hydrogels. *Chem. Soc. Rev.* **2012**, *41*, 6195−6214.

(18) Hoffman, A. S. Hydrogels for biomedical applications. *Adv. Drug Delivery Rev.* **2002**, *54*, 3−12.

(19) Tibbitt, M. W.; Anseth, K. S. Dynamic microenvironments: the fourth dimension. *Sci. Transl. Med.* **2012**, *4*, 160ps24.

(20) Fenton, O. S.; Olafson, K. N.; Pillai, P. S.; Mitchell, M. J.; Langer, R. Advances in Biomaterials for Drug Delivery. *Adv Mater Weinheim* **2018**, *30*, No. e1705328.

(21) Tibbitt, M. W.; Dahlman, J. E.; Langer, R. Emerging Frontiers in Drug Delivery. *J. Am. Chem. Soc.* **2016**, *138*, 704−717.

(22) Guvendiren, M.; Lu, H. D.; Burdick, J. A. Shear-thinning hydrogels for biomedical applications. *Soft Matter* **2012**, *8*, 260−272.

(23) Lopez Hernandez, H.; Grosskopf, A. K.; Stapleton, L. M.; Agmon, G.; Appel, E. A. Non-Newtonian Polymer-Nanoparticle Hydrogels Enhance Cell Viability during Injection. *Macromol. Biosci.* **2019**, *19*, 1800275.

(24) Webber, M. J.; Appel, E. A.; Meijer, E. W.; Langer, R. Supramolecular biomaterials. *Nat. Mater.* **2016**, *15*, 13−26.

(25) Appel, E. A.; Tibbitt, M. W.; Greer, J. M.; Fenton, O. S.; Kreuels, K.; Anderson, D. G.; Langer, R. Exploiting Electrostatic Interactions in Polymer-Nanoparticle Hydrogels. *ACS Macro Lett.* **2015**, *4*, 848−852.

(26) Lohmeijer, B. G. G.; Pratt, R. C.; Leibfarth, F.; Logan, J. W.; Long, D. A.; Dove, A. P.; Nederberg, F.; Choi, J.; Wade, C.; Waymouth, R. M.; Hedrick, J. L. Guanadine and Amidine Organocatalysts for Ring-Opening Polymerization of Cyclic Esters. *Macromolecules* **2006**, *39*, 8574−8583.
(27) Gref, R.; Minamitake, Y.; Peracchia, M.; Trubetskoy, V.; Torchilin, V.; Langer, R. Biodegradable long-circulating polymeric nanospheres. *Science* **1994**, *263*, 1600−1603.
(28) Kamaly, N.; Xiao, Z.; Valencia, P. M.; Radovic-Moreno, A. F.; Farokhzad, O. C. Targeted polymeric therapeutic nanoparticles: design, development and clinical translation. *Chem. Soc. Rev.* **2012**, *41*, 2971−3010.
(29) Cheng, J.; Teply, B.; Sherifi, I.; Sung, J.; Luther, G.; Gu, F.; Levynissenbaum, E.; Radovicmoreno, A.; Langer, R.; Farokhzad, O. Formulation of functionalized PLGA-PEG nanoparticles for in vivo targeted drug delivery. *Biomaterials* **2007**, *28*, 869−876.
(30) Appel, E. A.; Tibbitt, M. W.; Webber, M. J.; Mattix, B. A.; Veiseh, O.; Langer, R. Self-assembled hydrogels utilizing polymer-nanoparticle interactions. *Nat. Commun.* **2015**, *6*, 6295.
(31) Wischke, C.; Borchert, H. H. Fluorescein isothiocyanate labelled bovine serum albumin (FITC-BSA) as a model protein drug: opportunities and drawbacks. *Pharmazie* **2006**, *61*, 770−774.
(32) Ritger, P. L.; Peppas, N. A. A simple equation for description of solute release II: Fickian and anomalous release from swellable devices. *J. Controlled Release* **1987**, *5*, 37−42.
(33) Kim, J.; Li, W. A.; Choi, Y.; Lewin, S. A.; Verbeke, C. S.; Dranoff, G.; Mooney, D. J. Injectable, spontaneously assembling, inorganic scaffolds modulate immune cells in vivo and increase vaccine efficacy. *Nat. Biotechnol.* **2015**, *33*, 64−72.
(34) Vaahtomeri, K.; Brown, M.; Hauschild, R.; De Vries, I.; Leithner, A. F.; Mehling, M.; Kaufmann, W. A.; Sixt, M. Locally Triggered Release of the Chemokine CCL21 Promotes Dendritic Cell Transmigration across Lymphatic Endothelia. *Cell Rep.* **2017**, *19*, 902−909.


DOI: 10.1021/acs.biomac.9b01139